Chemosphere 290 (2022) 133331

Contents lists available at ScienceDirect

Chemosphere

journal homepage: www.elsevier.com/locate/chemosphere

Competitive inhibition of catalytic nitrate reduction over Cu–Pd-hematite by groundwater oxyanions

Nurbek Nurlan [a,1], Ainash Akmanova [a,1], Shanawar Hamid [b,*], Woojin Lee [a,c,**]

[a] Green Energy and Environmental Laboratory, National Laboratory Astana, Nazarbayev University, Nur-Sultan, 010000, Kazakhstan
[b] Environmental Sustainability Research Center, Department of Agricultural Engineering, Faculty of Engineering, Khwaja Fareed University of Engineering and Information Technology, Rahim Yar Khan, Pakistan
[c] Department of Civil and Environmental Engineering, School of Engineering and Digital Sciences, Nazarbayev University, Nur-Sultan, 010000, Kazakhstan

HIGHLIGHTS

- Evaluation of oxyanion influence on the catalytic NO_3^- reduction kinetics.
- Cl^-, PO_4^{3-}, BrO_3^- and SO_3^{2-} significantly inhibited the catalytic NO_3^- reduction.
- Inhibition effect of PO_4^{3-}, SO_3^{2-}, and BrO_3^- by competing for active catalytic sites.
- N_2 production remained unchanged with the addition of Cl^-, ClO_4^- and BrO_3^-
- N_2 selectivity increased with higher concentrations of SO_3^{2-}, SO_4^{2-} and PO_4^{3-}.

GRAPHICAL ABSTRACT

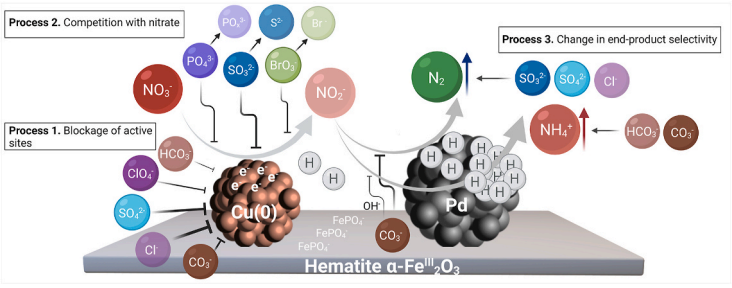

ARTICLE INFO

Handling editor: Hafiz M.N. Iqbal

Keywords:
Nitrate removal
Groundwater anions
Catalytic denitrification
Competitive inhibition
N_2 selectivity

ABSTRACT

The presence of various oxyanions in the groundwater could be the main challenge for the successive application of Cu–Pd-hematite bimetallic catalyst to aqueous NO_3^- reduction due to the inhibition of its catalytic reactivity and alteration of product selectivity. The batch experiments showed that the reduction kinetics of NO_3^- was strongly suppressed by ClO_4^-, PO_4^{3-}, BrO_3^- and SO_3^{2-} at low concentrations (>5 mg/L) and HCO_3^-, CO_3^{2-}, SO_4^{2-} and Cl^- at high concentrations (20–500 mg/L). The presence of anions significantly changing the end-product selectivities influenced high N_2 selectivity. The selectivity toward N_2 increased from 55% to 60%, 60%, and 70% as the concentrations of PO_4^{3-}, SO_3^{2-}, and SO_4^{2-} increased, respectively. It decreased from 55% to 35% in the presence of HCO_3^- and CO_3^{2-} in their concentration range of 0–500 mg/L. The production of NO_2^- was generally not detected, while the formation of NH_4^+ was observed as the second by-product. It was found that the presence of oxyanions in the NO_3^- reduction influenced the reactivity and selectivity of bimetallic catalysts by i) competing for active sites (PO_4^{3-}, SO_3^{2-}, and BrO_3^- cases) due to their similar structure, ii) blockage of the promoter and/or noble metal (HCO_3^-, CO_3^{2-}, SO_4^{2-}, Cl^- and ClO_4^- cases), and iii) interaction with the support surface (PO_4^{3-} case). The results can provide a new insight for the successful application of catalytic NO_3^- reduction technology with high N_2 selectivity to the contaminated groundwater system.

* Corresponding author.
** Corresponding author. Green Energy and Environmental Laboratory, National Laboratory Astana, Nazarbayev University, Nur-Sultan, 010000, Kazakhstan.
E-mail addresses: shanawar.hamid@kfueit.edu.pk (S. Hamid), woojin.lee@nu.edu.kz (W. Lee).
[1] Co-first authors.

https://doi.org/10.1016/j.chemosphere.2021.133331
Received 22 September 2021; Received in revised form 13 December 2021; Accepted 14 December 2021
Available online 16 December 2021

1. Introduction

Groundwater nitrate (NO_3^-) concentrations have been dramatically increasing due to the excessive use of fertilizers in agriculture and the continuous discharge of insufficiently treated industrial wastewater. High concentrations of NO_3^- in water bodies have posed severe concerns to ecological systems and human health. Consuming NO_3^- polluted water harmfully affects human health, resulting in blue baby syndrome, methemoglobinemia, and decreased oxygen-carrying capacity of hemoglobin (Keränen et al., 2015). Released nitrate could form carcinogenic nitrite (NO_2^-) and N-nitrosamine in contaminated aquatic environments, and therefore, its maximum allowable concentration was set to 10 mg/L by the United States Environmental Protection Agency (EPA) for potable water supply (Ahada and Suthar, 2018; Bhatnagar et al., 2010; Hamid et al., 2020b; Tokazhanov et al., 2020).

Various conventional water purification approaches, e.g., ion exchange, biological denitrification, adsorption, and reverse osmosis, have been investigated to date to treat NO_3^- efficiently (Bilidt, 1985; Fux et al., 2017; Hamid et al., 2020a; Holló and Czakó, 1987; Öztürk and Bektaş, 2005; Rezvani et al., 2019). However, catalytic NO_3^- reduction has emerged as promising technology due to its several salient features, e.g., fast reduction kinetics, high removal efficiency, no production of sludge, and selectivity to harmless end-product, nitrogen (N_2), compared to the conventional technologies (Soares et al., 2011, 2015; Wada et al., 2012). Experimental results from our recent studies have shown that NO_3^- can be reduced by bimetallic catalysts to >90% N_2 and ammonia (NH_4^+) as a negligible by-product (Hamid et al., 2017; Jung et al., 2012, 2014), and they were also stable and reusable for several cycles of catalytic NO_3^- reduction (Bae et al., 2016; Hamid et al., 2018). The catalytic NO_3^- reduction could fulfill the demand for an economically viable, eco-friendly, highly efficient, stable, and selective environmental technology to solve the impending NO_3^- contamination in natural and engineered water systems.

The application of NO_3^- reduction by bimetallic catalysts to contaminated groundwaters may have several challenges due to their inherent compositions, such as particulate matter and dissolved cations and anions. The threat of physical fouling by the adsorption of particulate matter on active catalyst sites has been frequently addressed in activated carbon-supported catalyst systems. Furthermore, soluble ions could be readily adsorbed on the catalyst surface and cause inhibition of catalytic reactions via surface poisoning and deactivation, which is much harder to remove from the catalyst surface. Thus, the real challenge of catalytic nitrate reduction in the contaminated groundwater would be the surface adsorption of the dissolved ions, especially anions (ClO_4^-, PO_4^{3-}, SO_4^{2-}, BrO_3^-, SO_3^{2-}, HCO_3^-, CO_3^{2-}, and Cl^-). However, no significant research has been conducted to investigate the effect of co-existing anions on the catalytic NO_3^- nitrate removal and their product selectivities (Soares et al., 2012). Published research papers mainly focused on the impact of the anions on simple NO_3^- removal efficiency. Still, they did not identify the relevant reaction mechanisms with groundwater anions, indicating that alterations/tailoring of the bimetallic catalysts and optimal operating conditions to address the challenge have not been fully achieved to date. Anions, especially oxyanions (ClO_4^-, PO_4^{3-}, SO_4^{2-}, BrO_3^-, SO_3^{2-}), have been termed water pollutants just like NO_3^- regulated by international environmental agencies (WHO, 2011), and their concentrations in groundwater range from a few mg/L to several hundred mg/L (Bae et al., 2020). The proper removal of oxyanions in groundwater systems has been a key environmental goal to purify and provide high-quality groundwater for various usages. Therefore, it is vital to investigate the removal of the oxyanions by bimetallic catalysts and identify their removal mechanism and by-products during the reaction. The study has been designed to carry out these experimental investigations to provide a basic understanding of the potential application of the catalytic nitrate reduction process for effective, selective, and versatile oxyanion removal in contaminated groundwater systems.

Recently, Cu–Pd bimetallic catalysts supported by hematite have shown an excellent performance in NO_3^- reduction due to its remarkable crystalline structure, uniform distribution of metals, high thermal stability, and reactivity (Hamid and Lee, 2016; Jung et al., 2014). Hematite (α- $Fe^{III}_2O_3$) is one of the most abundant iron-bearing soil minerals capable of removing environmental contaminants (Hashemzadeh et al., 2019; Liu et al., 2015; Shipley et al., 2013; Wu et al., 2013). The uniformly distributed metals on the hematite surface can effectively remove aqueous NO_3^- and significantly improve the selectivity of end-product even in actual groundwater application (Hamid and Lee, 2016). We selected Cu–Pd-hematite catalyst (Cu–Pd-hematite) as a representative bimetallic catalyst for the current study due to the properties mentioned above. The specific objectives were 1) to characterize NO_3^- reduction and investigate product selectivity in the presence of dissolved anions (ClO_4^-, PO_4^{3-}, SO_4^{2-}, BrO_3^-, SO_3^{2-}, HCO_3^-, CO_3^{2-}, and Cl^-) during the catalytic reaction by the Cu–Pd-hematite, and 2) to elucidate the primary reaction mechanism of competitive inhibition of the catalytic reduction during simultaneous removal of the oxyanions with target NO_3^-. We have conducted batch kinetic experiments to characterize the catalytic NO_3^- reduction with the high concentration of each oxyanion, evaluate the effect of oxyanion concentrations on the catalytic reaction, and investigate their by-product selectivity.

2. Materials and methods

2.1. Chemicals

The precursors for Cu and Pd to synthesize Cu–Pd-hematite were prepared by copper (II) chloride dihydrate (97.5%, Samchun Pure Chemical Co., Korea) and palladium (II) chloride (99.9%, Sigma–Aldrich Inc., USA). Pd precursor was dissolved in 0.5 M HCl (37%, Samchun Pure Chemical Co., Korea) to enhance its solubility. The prepared Cu–Pd-hematite was reduced before experimentation by 0.01 M sodium borohydride (98.0%, Samchun Pure Chemical Co., Korea) solution. The reagent grade sodium salts of oxyanions (i.e., sodium bicarbonate, sodium carbonate, sodium chloride, sodium phosphate, dibasic sodium sulfate, sodium sulfate, anhydrous sodium bromate, sodium perchlorate, and sodium sulfite) were used to prepare the stock solution of each oxyanion. The stock and standard solutions of NO_3^-, NO_2^- and NH_4^+ were prepared by potassium nitrate (99.0%, Duksan Pure Chemical Co., Korea), potassium nitrite (97.0%, Samchun Pure Chemical Co., Korea), and ammonium chloride (98.5%, Duksan Pure Chemical Co., Korea), respectively. Sodium bicarbonate (99.7%, Sigma-Aldrich Inc., USA) and sodium carbonate (99.5%, Sigma-Aldrich Inc., USA), and nitric acid (60%, Samchun Pure Chemical Co., Korea) were used to prepare an eluent for NO_3^-, NO_2^- and NH_4^+ determination via ion chromatography (IC). Deionized water (DIW) by ELGA PURELAB Classic system was purged with argon gas overnight to prepare deaerated deionized water (DDIW). The DDIW was used to prepare all chemical solutions and standards.

2.2. Catalyst synthesis

A previously optimized 2.2%Cu-1.6%Pd-hematite catalyst was prepared as reported in our previous work (Hamid and Lee, 2016; Jung et al., 2014). The catalyst was prepared by mixing 1.5 g hematite in 200 mL of DIW and ultra-sonicated for 6 min at room temperature. Next, Cu precursor solution was added by a drop into hematite solution and mechanically stirred for 120 min. Next, Pd precursor solution (1.6% Pd in 0.5 M HCl) was added by a drop into Cu-hematite solution and stirred for 120 min. Thus, prepared Cu–Pd hematite suspension was put in an oven at 105 °C for 24 h achieving complete drying. The oven-dried Cu–Pd-hematite was calcined at 350 °C for 120 min so that Cu and Pd precursors was stabilized on the hematite surface. The 2.2%Cu-1.6% Pd-hematite catalyst was added in DDIW and stirred to prepare a homogeneous mixture and was subsequently reduced by dropwise addition

of 0.01 M $NaBH_4$ solution. The reduced catalyst was filtered by a 0.2 μm membrane filter (Advantech, Japan), washed several times with DDIW to remove unwanted impurities, and transferred to the reactor system to remove nitrate in the catalyst suspension containing various oxyanions.

2.3. Experimental procedure of catalytic nitrate reduction

The batch kinetic experiment for the catalytic removal of NO_3^- in the presence of various oxyanions was performed in a 500 mL glass batch reactor as reported in our previous work (Hamid et al., 2018; Hamid and Lee, 2015; Jung et al., 2014). An amount of 215 mL DDIW was taken into the reactor and purged with H_2 gas to ensure anaerobic conditions. Then a 0.5 g of previously reduced 2.2%Cu-1.6%Pd−hematite was transferred to the reactor and dispersed by ultrasonication for 3 min. The respective amount of nitrate stock solution (20,000 mg/L as NO_3–N) and relative oxyanion stock solution was introduced into the reactor to start the catalytic reaction with oxyanions. CO_2 (30 mL/min) and H_2 (40 mL/min) gases were continuously supplied for buffering and reduction, respectively. We first characterized the catalytic removal of NO_3^- (30 mg/L) at a high concentration (100 mg/L) of each oxyanion (Cl^-, BrO_3^-, HCO_3^-, CO_3^{2-}, SO_3^{2-}, ClO_4^-, PO_4^{3-} SO_4^{2-}). Then, the effect of oxyanion concentrations (0, 100, 200, and 500 mg/L for Cl^-, HCO_3^-, CO_3^{2-}, SO_4^{2-}) and (0, 0.5, 1, 5 mg/L for SO_3^{2-}, BrO_3^-, ClO_4^-, and PO_4^{3-}) on the catalytic NO_3^- (30 mg/L) removal was evaluated, and their product selectivities were investigated during the reaction.

2.4. Analytical procedure

The concentrations of NO_3^-, NO_2^-, NH_4^+, and all other anions were determined by IC (883 basic IC plus, Metrohm, U.K.) equipped with a compact autosampler (863 Compact IC, Metrohm USA), anion columns (Metrosep A Supp 5–250/4.0 and Metrosep A Supp 7–250/4.0), and cation column (Metrosep C4-150/4.0) (Hamid et al., 2015, 2019; Hamid and Lee, 2015). The nitrate removal (R_{NO3}) and by-products selectivity ($S_{by\text{-}product}$) were calculated on a mass balance basis as given in the following equations.

$$R_{NO_3^-}(\%) = \frac{[NO_3^- - N]_i - [NO_3^- - N]_f}{[NO_3^- - N]} \quad (1)$$

$$S_{NO_2^-}(\%) = \frac{[NO_2^- - N]_f}{[NO_3^- - N]_i - [NO_3^- - N]_f} \quad (2)$$

$$S_{NH_4^+}(\%) = \frac{[NH_4^+ - N]_f}{[NO_3^- - N]_i - [NO_3^- - N]_f} \quad (3)$$

$$S_{N_2^-}(\%) = \frac{[NO_3^- - N]_i - [NO_3^- - N]_f - [NO_2^- - N]_f - [NH_4^+ - N]_f}{[NO_3^- - N]_i - [NO_3^- - N]_f} \quad (4)$$

where initial and final concentrations are denoted by subscripts *i* and *f*, respectively.

3. Results and discussion

3.1. Evaluation of the competitive inhibition of catalytic nitrate reduction by common groundwater oxyanions

Fig. 1(a) showed that the reaction kinetics of catalytic NO_3^- removal without oxyanions (control) was the fastest ($k = 0.05$ min^{-1}), and the catalytic reaction achieved 100% NO_3^- removal at the shortest time. In contrast, the response kinetics by the addition of anions can be divided into two distinct groups. One group (BrO_3^-, SO_3^{2-}, and PO_4^{3-}) strongly suppressed the catalytic NO_3^- reduction, while the other group (HCO_3^-, ClO_4^-, CO_3^{2-}, SO_4^{2-}, and Cl^-) slightly affected the reaction kinetics but did not seem to inhibit the catalytic reduction of NO_3^-. The nitrate reduction kinetics by HCO_3^- addition was similar to that by the control, demonstrating a complete NO_3^- removal at the same reaction time as the control. Likewise, the presence of ClO_4^-, CO_3^{2-} and SO_4^{2-} also moderately decreased the reaction rate, while Cl^- started to inhibit NO_3^- hydrogenation by diminishing the rate relatively much in the group. We can observe that the PO_4^{3-}, BrO_3^- and SO_3^{2-} significantly hindered the NO_3^- removal resulting in an incomplete NO_3^- removal in the reaction time. The reaction kinetics for the NO_3^- removal by Cu–Pd−hematite with the anions was negatively influenced in the order of $HCO_3^- < ClO_4^- < CO_3^{2-} < SO_4^{2-} < Cl^- < PO_4^{3-} < BrO_3^- < SO_3^{2-}$. To investigate the variations in the reaction kinetics, we monitored the aqueous concentrations of anions (SO_4^{2-}, Cl^-, PO_4^{3-}, BrO_3^-, SO_3^{2-}) and their potential by-products as well (Fig. 1(b)). The concentration of SO_3^{2-} decreased from 100 mg/L to ~70 mg/L over 400 min, showing that it could be adsorbed and slowly reduced as Eq. (5).

$$2SO_3^{2-} + 2H_2O + Cu \rightleftarrows S_2O_4^{2-} + 4OH^- + Cu^{2+} \quad (5)$$

Thus, the strong influence of SO_3^{2-} on the NO_3^- removal could be explained by preferential adsorption of SO_3^- or its by-products (Eq. (6)) on the reactive sites of Cu–Pd−hematite (Chaplin et al., 2006; Zhou et al., 2020).

$$SO_3^{2-} + 3H_2O + 3Cu \rightleftarrows S^{2-} + 6OH^- + 3Cu^{2+} \quad (6)$$

Irreversible adsorption of SO_3^- or S^{2-} on Pd could block the

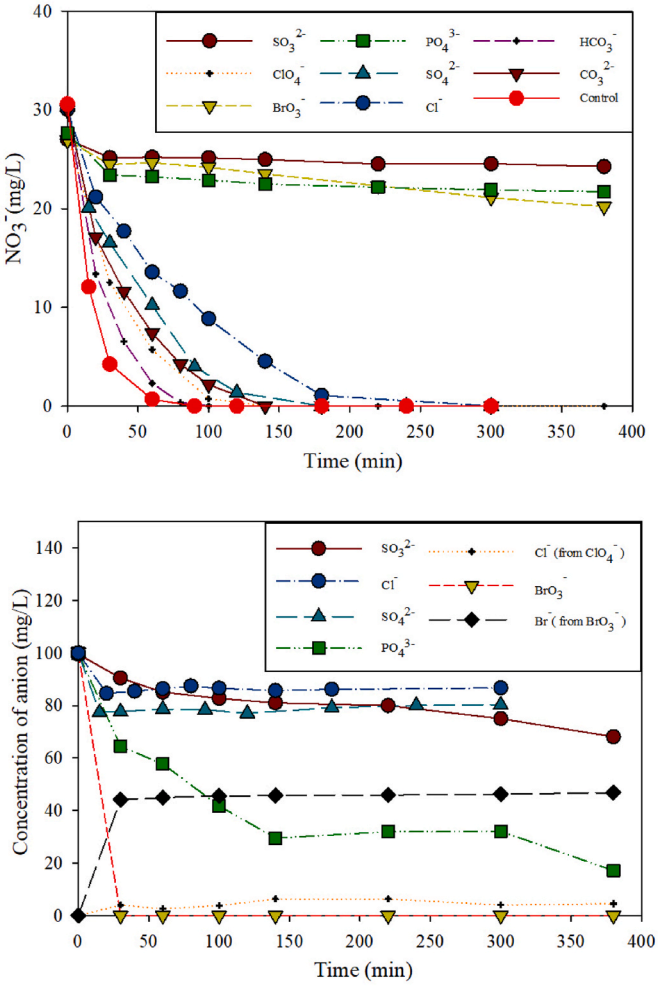

Fig. 1. The effect of anions (100 mg/L) on NO_3^- (30 mg/L) reduction by Cu–Pd−hematite (a), aqueous anion concentrations during their reduction/adsorption on the catalyst surface (b).

activation of H_2 and consequently, suppress the rejuvenation of Cu on the catalyst surface ($CuO + 2H_{ads} \rightarrow Cu^0 + H_2O$), leading to the inhibition of the continuously promoted NO_3^- reduction by Cu. Fig. 1(b) showed that ClO_4^- was slightly reduced to Cl^- as a final by-product (Eqs. (7) and (8)).

$$ClO_4^- + 8H^+ + 4Cu \rightarrow Cl^- + 4H_2O + 4Cu^{2+} \quad (7)$$

$$ClO_4^- \rightarrow ClO_3^- \rightarrow ClO_2^- \rightarrow ClO^- \rightarrow Cl^- \quad (8)$$

The sequential reductions of ClO_4^- during the NO_3^- removal can slow down the reaction kinetics by interfering with the reaction by its by-products resulting in 5 mg/L of its final aqueous concentration. The concentration of PO_4^{3-} decreased from 100 mg/L to ~15 mg/L throughout the reaction, and white precipitates (potentially $FePO_4$) were observed in the aqueous phase due probably to the soluble Fe(III) from the support (Tang et al., 2012; Zhou et al., 2020). This indicates that PO_4^{3-} could be removed via sequential sorption/precipitation/reduction to PO_2^{3-} and PO_3^{3-} during the NO_3^- removal, affecting the stability of the catalyst support (hematite) and interrupting the synergistic catalytic hydrogenation cycle of NO_3^-. The impact of PO_4^{3-} on the NO_3^- reduction could be caused by the formation of complexes at the hematite-water interface, hindering the contact of NO_3^- on the active catalyst sites. Despite the chemical interaction and electrostatic repulsion of NO_3^- from the Cu–Pd-hematite surface, BrO_3^- (3.51 Å) could compete with nitrate NO_3^- (3.35 Å) for the active catalytic reduction sites through the ion-sieve effect due to their similar size of hydrated ion radii (Nightingale, 1959). From the term of the effect, BrO_3^- could reach the catalyst's active sites depending on its ability to diffuse into the pores of the catalyst surface (Eliad et al., 2001; González et al., 2014; Jung et al., 2014). The concentration of BrO_3^- decreased entirely in 30 min and reduced to Br^-, indicating that BrO_3^- has a higher affinity towards Cu–Pd-hematite surface than slightly reduced NO_3^-. The higher affinity of adsorbed hydrogen (H_{ads}) to Cu(0) could also enhance the efficient reduction of BrO_3^-. Compared to the reduction of other oxyanions, BrO_3^- could be transformed to Br^- through the sequential reactions below.

$$BrO_3^- + 6H^+ + 3Cu^0 \rightarrow Br^- + 3H_2O + 3Cu^{2+} \quad (9)$$

$$BrO_3^- \rightarrow BrO_2^- \rightarrow BrO^- \rightarrow Br^- \quad (10)$$

It is important to note that NO_3^- was not reduced further after the complete removal of BrO_3^-, unlike a possible expectation that NO_3^- reduction continuously proceeds throughout the reaction time. The experimental result indicates that the by-product of BrO_3^- might also affect the catalytic NO_3^- removal throughout the reaction. According to the mass balance check by measuring Br^- concentration from BrO_3^- (Fig. 1(b)), it was not fully reduced to Br^- and/or its by-product could be adsorbed on the surface of Cu–Pd-hematite. A decrease in SO_4^{2-} concentration of ~20 mg/L during the reaction was observed, indicating a potential competitive affinity between SO_4^{2-} and NO_3^- for active catalytic sites of promoter metal (Soares et al., 2012). The results also imply that excessive SO_4^{2-} concentration may also poison noble metal (i.e., Pd) sites, thus suppressing H_2 activation activity and ultimately the reduction of NO_3^-. The concentration of Cl^- also decreased slightly to ~85 mg/L with a moderate NO_3^- removal, mainly caused by its adsorption on the Cu–Pd-hematite surface. It has been widely known that the Cl^- ions could readily erode metals on the catalyst surface leading to the moderate catalytic reduction kinetics by the decreased catalytic activity (Shen et al., 2020). Based on the experimental results, we further evaluated the effect of various groundwater anion concentrations on the selectivity of products during the catalytic nitrate removal.

3.2. Effect of oxyanion concentrations on the catalytic nitrate removal kinetics and by-product selectivity

3.2.1. Effect of SO_3^{2-}

As shown in Fig. 2, the various concentrations of SO_3^{2-} (0, 0.5, 1, and 5 mg/L) demonstrated different effects on the catalytic NO_3^- removal by Cu–Pd−hematite. The inhibitory effect of SO_3^{2-} was remarkable at the highest concentration (5 mg/L), showing the decelerated catalytic NO_3^- reduction kinetics ($k = 0.04$ min^{-1}). At lower SO_3^{2-} concentrations ranging from 0 to 1 mg/L, only a slight or no influence on the reaction kinetics can be observed compared to that of control ($k = 0.05$ min^{-1}). The catalytic NO_3^- removal is a multi-step reaction process. NO_3^- was initially reduced to NO_2^- on the surface of Cu promoter metal, and then NO_2^- was further reduced to NH_4^+ and N_2 on the surface of Cu–Pd bimetallic particles, i.e., $2NO_2^- + 12H_{ads}$-Pd(0) → Pd(0) + $2NH_4^+ + 4OH^-$ and $2NO_2^- + 4H_{ads}$-Pd(0) → Pd(0) + $N_2 + 4OH^-$ [15,29]. The presence of SO_3^{2-} can significantly alter the reaction mechanism by affecting the reduction of NO_3^- to NO_2^- ($NO_3^- + Cu(0) \rightarrow Cu(II)O + NO_2^-$) (Hamid et al., 2015). The Cu particles on the catalyst could be exposed to SO_3^{2-} and eroded (Eqs. (5) and (6)), resulting in an irregular and insufficient contact of NO_3^- with H_{ads} on the promoter metal sites. This leads to slow catalytic reaction kinetics and incomplete NO_3^- removal in the presence of SO_3^{2-}. We can observe NH_4^+ and N_2 as products during the catalytic NO_3^- removal but cannot detect NO_2^- in the catalyst suspension with SO_3^{2-}. The spillover H_{ads} from active Pd sites reduced promoter metal oxides and subsequently NO_2^- to further reduced species. Because the continuous consumption of H_{ads} by promoter metal oxides and NO_2^- could also decrease H_{ads} supply, the NH_4^+ selectivity in the catalyst suspension with SO_3^{2-} decreased as the increase of its concentration, i.e., 55% at 0.5 and 1 mg/L and 40% at 5 mg/L. The limited availability of H_2 could enhance the probability of N–N recombination to form gaseous N_2. Thus, the formation of N_2 demonstrated an opposite trend showing its maximum selectivity (60%) at the highest SO_3^{2-} concentration. The effect of SO_3^{2-} concentration on the reaction kinetics and product selectivity can be mainly attributed to the contents of Cu sites and H_{ads} affected by the increase of its concentration, resulting in the limiting reaction conditions and leading to the slow reaction kinetics and high N_2 selectivity.

3.2.2. Effect of SO_4^{2-}

Fig. 3 showed that NO_3^- reduction kinetics was more significantly affected by different SO_4^{2-} concentrations (100, 200, and 500 mg/L) than that by the control. The rate constant of the catalytic reaction substantially decreased from 0.05 min^{-1} to 0.013 min^{-1} as the SO_4^{2-} concentration increased from 0 mg/L to 500 mg/L. The inhibitory effects of SO_4^{2-} concentration on the reaction kinetics could be explained

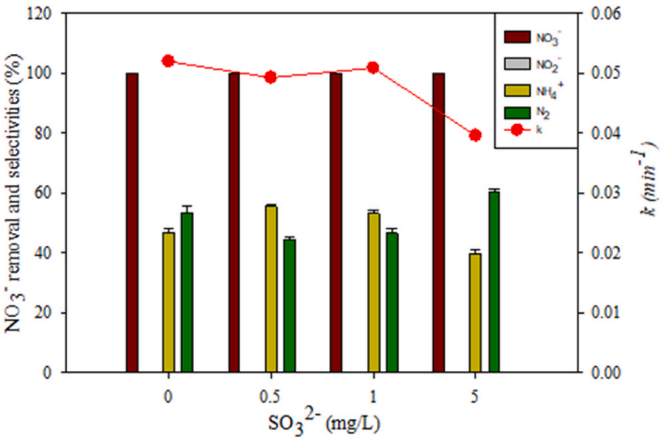

Fig. 2. Catalytic nitrate reduction by Cu–Pd-hematite with different concentrations of SO_3^{2-}.

by the competition between NO_3^- and SO_4^{2-} for the active Cu sites at the first step of catalytic NO_3^- reduction to NO_2^-. The selectivities towards NH_4^+ and N_2 varied within the range of SO_4^{2-} concentrations. The selectivity of NH_4^+ dropped from 55% to ~30% with the increase of SO_4^{2-} concentration, whereas N_2 selectivity was more enhanced. The highest N_2 formation (70%) was observed at the highest SO_4^{2-} concentration (500 mg/L), and at lower SO_4^{2-} concentrations, it was even lower than 55%. Therefore, the presence of SO_4^{2-} anions has also promoted the formation of N_2 with favorable removal efficiency, even though the kinetic rate has decreased. We cannot detect NO_2^- formation during the reactions at different SO_4^{2-} concentrations. It could be assumed that NO_2^- was wholly and instantaneously reduced to N_2 and NH_4^+ under the experimental conditions. As discussed above, the SO_4^{2-} could cause a poor activated hydrogen condition on the catalyst surface, as shown in the SO_3^{2-} case, leading to the higher N_2 selectivity. Therefore, SO_4^{2-} might promote the instantaneous NO_2^- reduction on Pd active sites and fast consumption of spillover H_{ads} for the rejuvenation of Cu(II)O resulting in low H_{ads} and high N_{ads} concentrations on the Cu–Pd-hematite surface.

3.2.3. Effect of CO_3^{2-}

The influence of different concentrations of CO_3^{2-} on the NO_3^- reduction kinetics was demonstrated in Fig. 4. As the loading of CO_3^{2-} in the suspension increased to 20 mg/L, the kinetic rate constant of NO_3^- reduction abruptly decreased from 0.055 to 0.027 min^{-1}, and its decline was gradually continued and reached 0.01 min^{-1} at 500 mg/L, which is six times lower than the rate constant of the control. The catalytic NO_3^- reduction kinetic was negatively affected by the increase of CO_3^{2-} concentrations due to the dual inhibitory effect on the promoter and noble metals during the NO_3^- reduction. Carbonate having an identical planar structure of NO_3^- could inhibit the catalytic NO_3^- reduction to NO_2^- on the active surface of Cu. It is noteworthy that the formation of a negligible amount of NO_2^- was observed at the highest CO_3^{2-} concentration, while no NO_2^- formation was observed throughout the catalytic NO_3^- reductions with other oxyanions. It has been widely reported that CO_3^{2-} decelerated the reaction kinetics and ultimately ceased the reduction of NO_2^- to N_2 and NH_4^+ by blocking the active sites of Pd with hydroxide ions at high pH (Lubphoo et al., 2015; Prüsse and Vorlop, 2001). Therefore, the increase of CO_3^{2-} might inhibit the catalytic NO_3^- reduction mechanisms and decrease its removal rates to a moderate extent in general. Fig. 4 also showed that NH_4^+ selectivity increased gradually from 43% and then saturated to 63% with the increase of CO_3^{2-} concentration to 500 mg/L, whereas the N_2 selectivity decreased accordingly (60%–39%). The excessive amount of accumulated hydrogen molecules at active sites of Pd led to the formation of NH_4^+ rather than N_2 as the main product.

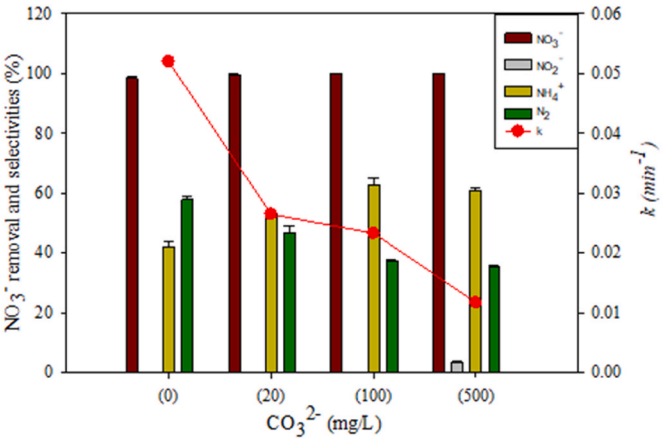

Fig. 4. Catalytic nitrate reduction by Cu–Pd-hematite with different concentrations of CO_3^{2-}.

3.2.4. Effect of HCO_3^-

Bicarbonate did not demonstrate a strong impact on the catalytic NO_3^- removal compared to other groundwater oxyanions, as shown in Fig. 1(a). Fig. 5 showed the effect of HCO_3^- concentrations (0–500 mg/L) on the catalytic NO_3^- reduction in the Cu–Pd−hematite suspensions. As the concentration of HCO_3^- increased to 100 mg/L, the kinetic rate constant of catalytic NO_3^- reduction decreased to 0.025 min^{-1} and further dropped down to 0.012 min^{-1} at 500 mg/L, demonstrating an inversely-proportional linear relationship throughout the reaction. We cannot observe NO_2^- formation in the catalyst suspensions with HCO_3^- during the reaction either. Although the catalytic NO_3^- reduction system was buffered with CO_2, we can observe the increase of the suspension pH from 5.5 to 6.5 during the reaction. The competitive inhibition mechanism by HCO_3^- during the catalytic NO_3^- removal and HCO_3^- effect on the selectivity of N_2 and NH_4^+ were similar to CO_3^{2-}. As the concentration of HCO_3^- increased (0 mg/L to 500 mg/L), the selectivity toward N_2 proportionally decreased (58%–33%), and NH_4^+ selectivity increased (42%–67%), respectively. A similar result has been reported for the catalytic NO_3^- reduction by Pd–Cu bimetallic catalyst supported on hydrotalcite mineral, showing the decrease in the selectivity towards N_2 in the presence of HCO_3^- (Wang et al., 2007). The results indicate that the high concentration of HCO_3^- affected both Cu–Pd-hematite reactivity and its product selectivity. It deactivated the reactive Cu sites responsible for reducing NO_3^- ($NO_3^- + Cu(0) \rightarrow Cu(II)O + NO_2^-$), ultimately causing the deceleration in NO_3^- reduction kinetics and promoted the formation of harmful NH_4^+ and demoted N_2

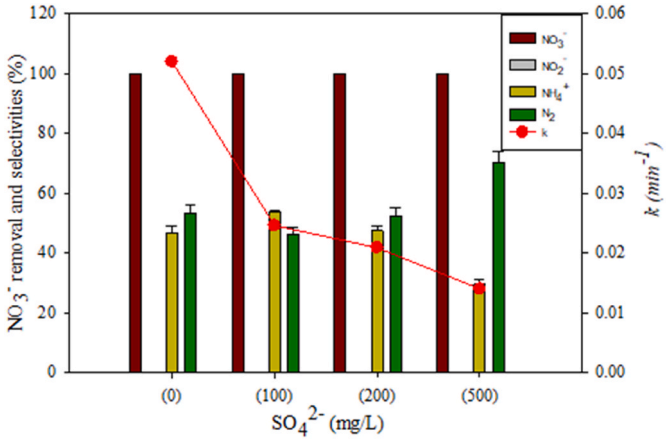

Fig. 3. Catalytic nitrate reduction by Cu–Pd-hematite with different concentrations of SO_4^{2-}.

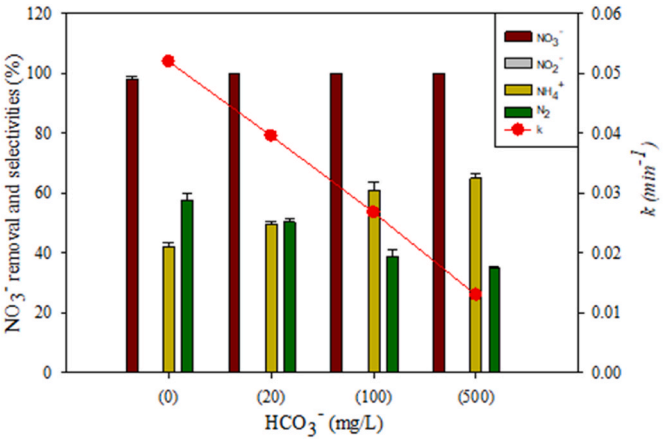

Fig. 5. Catalytic nitrate reduction by Cu–Pd-hematite with different concentrations of HCO_3^-.

formation correspondingly by the increase of the catalyst suspension pH even under the buffer system.

3.2.5. Effect of ClO_4^-

Fig. 6 showed catalytic NO_3^- removal and product selectivity profiles at four different dissolved ClO_4^- concentrations (0, 0.5, 1, and 5 mg/L). The reaction kinetics demonstrated a slight decrease at the lowest ClO_4^- concentration (0.5 mg/L); however, its decline was steadily accelerated by higher ClO_4^- concentrations, i.e., twice higher (0.03 min^{-1}) at 5 mg/L. To understand the negative effect of ClO_4^- concentration on the deteriorated catalytic performance of Cu–Pd-hematite, we monitored and analyzed the concentration of Cl^- ions in the catalyst suspension. Such a drop in the catalytic activity of Cu–Pd-hematite could be due mainly to the formation of Cl^- resulting from the ClO_4^- reduction (Eq. (7)) during the catalytic NO_3^- removal. According to Fig. 1(b), the formation of Cl^- ions can be confirmed by the concentration profile of Cl^- from ClO_4^- addition. It has been widely known that Cl^- is one of the common competitive inhibitors for the active catalyst sites during the catalytic NO_3^- reduction. We performed an additional experiment to investigate the detailed effect of Cl^- concentration, which is discussed in the next section (3.2.6). Moreover, NO_2^- was not detected during the reaction and might be continuously and instantaneously reduced to N_2 or NH_4^+. The product selectivities towards N_2 and NH_4^+ did not change much with the increase of ClO_4^- concentration. At the highest ClO_4^- concentration (5 mg/L), we can observe a slight decrease in N_2 selectivity and a corresponding minor increase in NH_4^+ selectivity by 10% of those from the control experiment, respectively.

3.2.6. Effect of Cl^-

The effect of Cl^- on the catalytic NO_3^- reduction by Cu–Pd-hematite was demonstrated in Fig. 7. The catalytic NO_3^- removal was strongly affected by Cl^- concentration. As the concentration of Cl^- increased to 100 mg/L, the reaction kinetics was significantly decelerated, leading to a sharp decrease in the rate constant to 0.022 min^{-1}. Higher concentrations of Cl^- (250 and 500 mg/L) further deteriorated the catalytic NO_3^- reduction kinetics, resulting in 13 times decrease in rate kinetics (0.005 min^{-1}) at 500 mg/L. The significant decline of NO_3^- reduction could be caused by the substantial inhibition effect of Cl^- on the active Cu sites for the NO_3^- reduction to NO_2^-. Indeed, the promoter metal can be eroded from the catalyst surface to bulk solution with Cl^- ions and decrease Cu content on the Cu–Pd-hematite surface. As shown in Fig. 7, the formation of NO_2^- was not observed throughout the catalytic reaction. Additionally, an enhancement in N_2 selectivity can be noticed from 60% to ~70% with the increase of Cl^- concentration, while NH_4^+ selectivity slightly decreased by 5% of the control. The selectivity trend

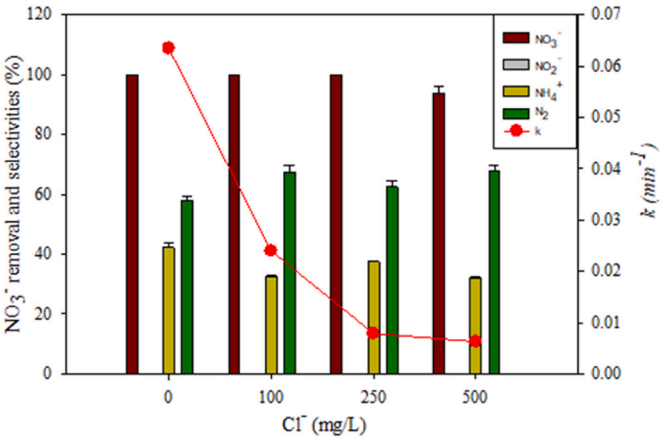

Fig. 7. Catalytic nitrate reduction by Cu–Pd-hematite with different concentrations of Cl^-.

contradicts the experimental result from the literature with the activated carbon and hydrotalcite supported Pd–Cu catalyst showing ammonium and nitrite accumulations by Cl^- ions during the catalytic reaction (Wang et al., 2007, 2009). The enhanced N_2 selectivity is due to the hematite property, which provides appropriate sites for depositing bimetals that possess the closest distance between Pd and Cu sites.

3.2.7. Effect of BrO_3^-

Fig. 8 demonstrated the catalytic NO_3^- removal and product selectivity on Cu–Pd-hematite with different BrO_3^- concentrations. The high concentration of BrO_3^- (100 mg/L) significantly inhibited the NO_3^- reduction resulting in the considerably deteriorated reaction kinetics with incomplete removal (Fig. 1(a)); however, when the lower BrO_3^- concentrations were introduced to the catalyst suspension, the kinetic rate constant slightly and gradually decreased to 0.058 min^{-1} by 1 mg/L. An increase of BrO_3^- concentration to 5 mg/L showed a remarkable decline of the rate constant (0.045 min^{-1}) without NO_2^- formation during the whole reaction period. The results could be attributed to the competitive inhibition of BrO_3^- (Eq. (9)) for the reactive surface sites of Cu–Pd-hematite due to the structural similarities (ionic radius) between BrO_3^- and NO_3^-. As illustrated in Fig. 1(b), BrO_3^- was entirely removed in the catalyst suspension, and ~42% of it was reduced to Br^- during the reaction. The product Br^- could competitively and irreversibly inhibit the catalytic NO_3^- reduction to NO_2^- demonstrating a strong negative impact. In addition, the selectivities towards N_2 and NH_4^+ did not change much as the increase of BrO_3^- concentration, showing similar selectivities of the control test. The results also indicate that BrO_3^- is a

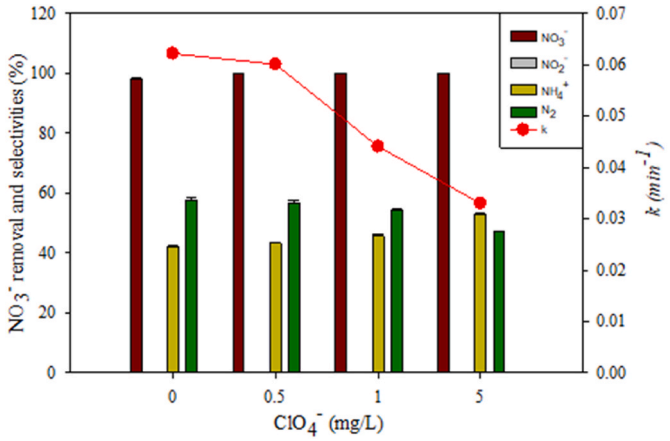

Fig. 6. Catalytic nitrate reduction by Cu–Pd-hematite with different concentrations of ClO_4^-.

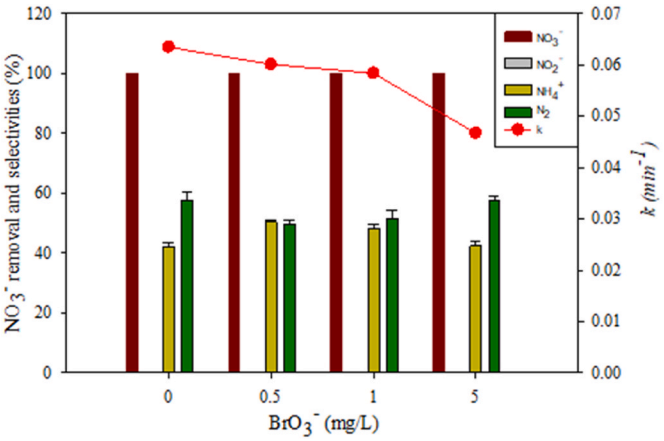

Fig. 8. Catalytic nitrate reduction by Cu–Pd-hematite with different concentrations of BrO_3^-

potent inhibitor at relatively higher concentrations (e.g., >100 mg/L).

3.2.8. Effect of PO_4^{3-}

The catalytic NO_3^- removal was strongly and negatively influenced by the high PO_4^{3-} concentration (100 mg/L), as shown in Fig. 1(a). Fig. 9 further demonstrated its influence on the reaction at lower PO_4^{3-} concentrations (0–5 mg/L). The PO_4^{3-} having both symmetric and asymmetric tetrahedral structures, has been widely known to interact with metal oxide surfaces readily. Thus, PO_4^{3-} adsorbed on the surface of Cu–Pd-hematite could significantly inhibit the reduction of NO_3^- to NO_2^- on the active promoter surface (Kang et al., 2011). The experimental result also showed that the inhibitory effect on the reaction kinetics was more significant with increasing the PO_4^{3-} concentration at the lower level. As the concentration of PO_4^{3-} increased to 0.5 mg/L, the kinetics rate constant decreased considerably from 0.065 to 0.035 min^{-1}, and the subsequent decrease of the rate constant can be continuously observed by 5 mg/L concentration (0.02 min^{-1}). It is suggested that the PO_4^{3-} could cause permanent surface deactivation of the catalyst by competitive adsorption on the active surfaces of metallic catalysts (e.g.) (Prüsse and Vorlop, 2001). No NO_2^- formation was observed during the reaction, and selectivities towards NH_4^+ and N_2 were similar to those of the control even with the increase of PO_4^{3-} concentration.

4. Conclusion

In this study, the results from catalytic denitrification experiments at high oxyanion concentration (100 mg/L) showed that the inhibition effect of co-existing oxyanions on the catalytic NO_3^- removal differed, and its extent followed the order; $HCO_3^- < ClO_4^- < CO_3^{2-} < SO_4^{2-} < Cl^- < PO_4^{3-} < BrO_3^- < SO_3^{2-}$. We can also observe that some oxyanions played a competitive inhibitor role at lower concentration levels, while others only can do at the higher level. The novel findings suggest that the inhibitory effect of Cl^-, PO_4^{3-}, BrO_3^- and SO_3^{2-} on the catalytic NO_3^- reduction needs to be seriously considered for its proper application to catalytic nitrate remediation of anion enriched groundwater and soil to avoid the slow reaction kinetics and incomplete NO_3^- removal. To the best of our knowledge, this study is the first report revealing the influence of groundwater oxyanion concentrations on the product selectivity during the catalytic NO_3^- reduction. The results highlight that the product selectivity during the catalytic NO_3^- reduction was also influenced by the variations of oxyanion concentrations. The selectivity towards N_2 during the NO_3^- reduction decreased significantly as HCO_3^-, CO_3^{2-}, and ClO_4^- concentrations increased. However, it increased as SO_3^{2-}, SO_4^{2-} and PO_4^{3-} concentrations increased. The Cu–Pd-hematite showed remarkable continuous NO_3^- reduction with good selectivities towards N_2 and NH_4^+ in the presence of the oxyanions, and the formation of NO_2^- can only be observed with CO_3^{2-} at 500 mg/L, due possibly to the poisoning of the Pd catalyst. We identified the subsequent reaction mechanisms for the catalytic NO_3^- reduction and product selectivity in the presence of the oxyanions, including competitive inhibition, blockage of promotor metal, change of reaction condition (i.e., suspension pH increase), and reaction with the support surface. The outcome of this study can improve the fundamental understanding of catalytic NO_3^- reduction technology for the remediation of contaminated groundwater and soil with abundant competing anions and help provide novel solutions for its proper application to the remediation sites and optimal operation of the catalytic removal system.

Credit author statement

Nurbek Nurlan: Investigation, Methodology, writing original draft, Visualization. Ainash Akmanova: Investigation, Methodology, writing original draft, Visualization. Shanawar Hamid: Conceptualization, Formal analysis, Methodology, reviewing the manuscript. Woojin Lee: Supervision, Conceptualization, writing and reviewing the manuscript,

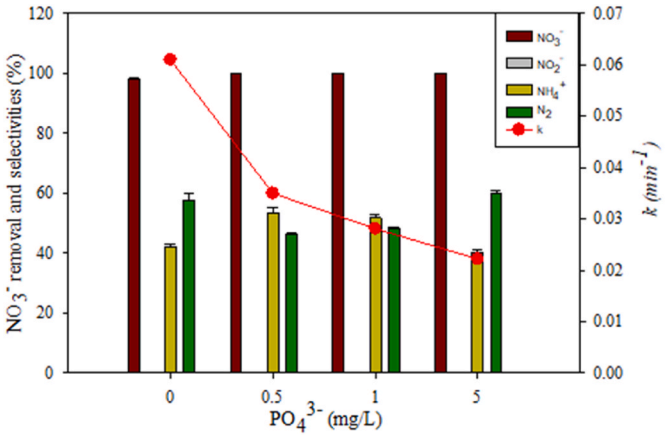

Fig. 9. Catalytic nitrate reduction by Cu–Pd-hematite with different concentrations of PO_4^{3-}

Funding acquisition

Declaration of competing interest

The authors declare that they have no known competing financial interests or personal relationships that could have appeared to influence the work reported in this paper.

Acknowledgments

This study has been supported by the Research Grants of Nazarbayev University (091019CRP2106 and 021220FD1051) and the Ministry of Education and Science of the Republic of Kazakhstan (APO9260229). The authors would like to thank the anonymous reviewers who helped significantly improve the quality of the paper.

References

Ahada, C.P.S., Suthar, S., 2018. Groundwater nitrate contamination and associated human health risk assessment in southern districts of Punjab, India. Environ. Sci. Pollut. Res. 25, 25336–25347. https://doi.org/10.1007/s11356-018-2581-2.

Bae, S., Hamid, S., Jung, J., Sihn, Y., Lee, W., 2016. Effect of promoter and noble metals and suspension pH on catalytic nitrate reduction by bimetallic nanoscale Fe^0 catalysts. Environ. Technol. 37, 1077–1087. https://doi.org/10.1080/09593330.2015.1101166.

Bae, S., Yoon, S., Kaplan, U., Kim, H., Han, S., Lee, W., 2020. Effect of groundwater ions (Ca^{2+}, Na^+, and HCO_3^-) on removal of hexavalent chromium by Fe(II)-phosphate mineral. J. Hazard Mater. 398 https://doi.org/10.1016/j.jhazmat.2020.122948.

Bhatnagar, A., Kumar, E., Sillanpää, M., 2010. Nitrate removal from water by nano-alumina: characterization and sorption studies. Chem. Eng. J. 163, 317–323. https://doi.org/10.1016/j.cej.2010.08.008.

Bilidt, H., 1985. The use of reverse osmosis for removal of nitrate in drinking water. Desalination 53, 225–230. https://doi:10.1016/00119164(85)85063-3.

Chaplin, B.P., Roundy, E., Guy, K.A., Shapley, J.R., Werth, C.I., 2006. Effects of natural water ions and humic acid on catalytic nitrate reduction kinetics using an alumina supported Pd-Cu catalyst. Environ. Sci. Technol. 40, 3075–3081. https://doi.org/10.1021/es0525298.

Eliad, L., Salitra, G., Soffer, A., Aurbach, D., 2001. Ion sieving effects in the electrical double layer of porous carbon electrodes: estimating effective ion size in electrolytic solutions. J. Phys. Chem. B 105, 6880–6887. https://doi.org/10.1021/jp010086y.

Fux, I., Birnhack, L., Tang, S.C.N., Lahav, O., 2017. Removal of nitrate from drinking water by ion-exchange followed by nzvi-based reduction and electrooxidation of the ammonia product to n2(G). ChemEngineering 1, 1–19. https://doi.org/10.3390/chemengineering1010002.

González, M.A., Pavlovic, I., Rojas-Delgado, R., Barriga, C., 2014. Removal of Cu^{2+}, Pb^{2+} and Cd^{2+} by layered double hydroxide-humate hybrid. Sorbate and sorbent comparative studies. Chem. Eng. J. 254, 605–611. https://doi.org/10.1016/j.cej.2014.05.132.

Hamid, S., Abudanash, D., Han, S., Kim, J.R., Lee, W., 2019. Strategies to enhance the stability of nanoscale zero-valent iron (NZVI) in continuous BrO_3^- reduction. J. Environ. Manag. 231, 714–725. https://doi.org/10.1016/j.jenvman.2018.10.026.

Hamid, S., Bae, S., Lee, W., 2018. Novel bimetallic catalyst supported by red mud for enhanced nitrate reduction. Chem. Eng. J. 348, 877–887. https://doi.org/10.1016/j.cej.2018.05.016.

Hamid, S., Bae, S., Lee, W., Amin, M.T., Alazba, A.A., 2015. Catalytic nitrate removal in continuous bimetallic Cu-Pd/nanoscale zerovalent iron system. Ind. Eng. Chem. Res. 54, 6247–6257. https://doi.org/10.1021/acs.iecr.5b01127.

Hamid, S., Golagana, S., Han, S., Lee, G., Babaa, M.R., Lee, W., 2020a. Stability of Sn–Pd-Kaolinite catalyst during heat treatment and nitrate reduction in continuous flow reaction. Chemosphere 241, 125115. https://doi.org/10.1016/j.chemosphere.2019.125115.

Hamid, S., Kumar, M.A., Han, J.I., Kim, H., Lee, W., 2017. Nitrate reduction on the surface of bimetallic catalysts supported by nano-crystalline beta-zeolite (NBeta). Green Chem. https://doi.org/10.1039/c6gc02349e.

Hamid, S., Lee, W., 2016. Reduction of nitrate in groundwater by hematite supported bimetallic catalyst. Adv. Environ. Res. 5, 51–59. https://doi.org/10.12989/aer.2016.5.1.051.

Hamid, S., Lee, W., 2015. Nitrate reduction by iron supported bimetallic catalyst in low and high nitrogen regimes. Adv. Environ. Res. 4, 263–271. https://doi.org/10.12989/aer.2015.4.4.263.

Hamid, S., Niaz, Y., Bae, S., Lee, W., 2020b. Support induced influence on the reactivity and selectivity of nitrate reduction by Sn-Pd bimetallic catalysts. J. Environ. Chem. Eng. 8, 103754. https://doi.org/10.1016/j.jece.2020.103754.

Hashemzadeh, M., Nilchi, A., Hassani, A.H., 2019. Synthesis of novel surface-modified hematite nanoparticles for lead ions removal from aqueous solution. Mater. Chem. Phys. 227, 279–290. https://doi.org/10.1016/j.matchemphys.2019.02.025.

Holló, J., Czakó, L., 1987. Nitrate removal from drinking water in a fluidized-bed biological denitrification bioreactor. Acta Biotechnol. 7, 417–423. https://doi:10.1002/abio.370070509.

Jung, J., Bae, S., Lee, W., 2012. Nitrate reduction by maghemite supported Cu-Pd bimetallic catalyst. Appl. Catal. B Environ. 127, 148–158. https://doi.org/10.1016/j.apcatb.2012.08.017.

Jung, S., Bae, S., Lee, W., 2014. Development of Pd-Cu/hematite catalyst for selective nitrate reduction. Environ. Sci. Technol. 48, 9651–9658. https://doi.org/10.1021/es502263p.

Kang, S.A., Li, W., Lee, H.E., Phillips, B.L., Lee, Y.J., 2011. Phosphate uptake by TiO_2: batch studies and NMR spectroscopic evidence for multisite adsorption. J. Colloid Interface Sci. 364, 455–461. https://doi.org/10.1016/j.jcis.2011.07.088.

Keränen, A., Leiviskä, T., Hormi, O., Tanskanen, J., 2015. Removal of nitrate by modified pine sawdust: effects of temperature and co-existing anions. J. Environ. Manag. 147, 46–54. https://doi.org/10.1016/j.jenvman.2014.09.006.

Liu, A., Zhou, W., Shen, K., Liu, J., Zhang, X., 2015. One-pot hydrothermal synthesis of hematite-reduced graphene oxide composites for efficient removal of malachite green from aqueous solution. RSC Adv. 5, 17336–17342. https://doi.org/10.1039/c4ra15589k.

Lubphoo, Y., Chyan, J.M., Grisdanurak, N., Liao, C.H., 2015. Nitrogen gas selectivity enhancement on nitrate denitrification using nanoscale zero-valent iron supported palladium/copper catalysts. J. Taiwan Inst. Chem. Eng. 57, 143–153. https://doi.org/10.1016/j.jtice.2015.05.005.

Nightingale, E.R., 1959. Phenomenological theory of ion solvation. Effective radii of hydrated ions. J. Phys. Chem. 63, 1381–1387. https://doi.org/10.1021/j150579a011.

Öztürk, N., Bektaş, T.E., 2005. Reply to comment on "Nitrate removal from aqueous solution by adsorption onto various materials". Y.S. Ho. J. Hazard. Mater. 120, 277. https://doi.org/10.1016/j.jhazmat.2005.01.008.

Prüsse, U., Vorlop, K.D., 2001. Supported bimetallic palladium catalysts for water-phase nitrate reduction. J. Mol. Catal. A Chem. 173, 313–328. https://doi.org/10.1016/S1381-1169(01)00156-X.

Rezvani, F., Sarrafzadeh, M.H., Ebrahimi, S., Oh, H.M., 2019. Nitrate removal from drinking water with a focus on biological methods: a review. Environ. Sci. Pollut. Res. 26, 1124–1141. https://doi.org/10.1007/s11356-017-9185-0.

Shen, Z., Liu, D., Dong, X., Shi, J., Ma, Y., Fan, J., Zhang, L., 2020. Nitrate reduction using iron and copper bimetallic nanoparticles supported by chelating resin: effect of solution chemistry, mechanism, and regeneration. J. Environ. Eng. 146, 04020011 https://doi.org/10.1061/(asce)ee.1943-7870.0001671.

Shipley, H.J., Engates, K.E., Grover, V.A., 2013. Removal of Pb(II), Cd(II), Cu(II), and Zn (II) by hematite nanoparticles: effect of sorbent concentration, pH, temperature, and exhaustion. Environ. Sci. Pollut. Res. 20, 1727–1736. https://doi.org/10.1007/s11356-012-0984-z.

Soares, O.S.G.P., Marques, L., Freitas, C.M.A.S., Fonseca, A.M., Parpot, P., Órfão, J.J.M., Pereira, M.F.R., Neves, I.C., 2015. Mono and bimetallic NaY catalysts with high performance in nitrate reduction in water. Chem. Eng. J. 281, 411–417. https://doi.org/10.1016/j.cej.2015.06.093.

Soares, O.S.G.P., Órfão, J.J.M., Pereira, M.F.R., 2011. Nitrate reduction with hydrogen in the presence of physical mixtures with mono and bimetallic catalysts and ions in solution. Appl. Catal. B Environ. 102, 424–432. https://doi.org/10.1016/j.apcatb.2010.12.017.

Soares, O.S.G.P., Órfo, J.J.M., Gallegos-Suarez, E., Castillejos, E., Rodríguez-Ramos, I., Pereira, M.F.R., 2012. Nitrate reduction over a Pd-Cu/MWCNT catalyst: application to a polluted groundwater. Environ. Technol. 33, 2353–2358. https://doi.org/10.1080/09593330.2012.668945.

Tang, C., Zhang, Z., Sun, X., 2012. Effect of common ions on nitrate removal by zero-valent iron from alkaline soil. J. Hazard Mater. 231–232, 114–119. https://doi.org/10.1016/j.jhazmat.2012.06.042.

Tokazhanov, G., Ramazanova, E., Hamid, S., Bae, S., Lee, W., 2020. Advances in the catalytic reduction of nitrate by metallic catalysts for high efficiency and N_2 selectivity: a review. Chem. Eng. J. 384, 123252. https://doi.org/10.1016/j.cej.2019.123252.

Wada, K., Hirata, T., Hosokawa, S., Iwamoto, S., Inoue, M., 2012. Effect of supports on Pd-Cu bimetallic catalysts for nitrate and nitrite reduction in water. Catal. Today 185, 81–87. https://doi.org/10.1016/j.cattod.2011.07.021.

Wang, Y., Qu, J., Liu, H., 2007. Effect of liquid property on adsorption and catalytic reduction of nitrate over hydrotalcite-supported Pd-Cu catalyst. J. Mol. Catal. A Chem. 272, 31–37. https://doi.org/10.1016/j.molcata.2007.02.028.

Wang, Y., Sakamoto, Y., Kamiya, Y., 2009. Remediation of actual groundwater polluted with nitrate by the catalytic reduction over copper–palladium supported on active carbon. Appl. Catal. A-Gen. 361, 123–129. https://doi:10.1016/j.apcata.2009.04.006.

WHO, 2011. Guidelines for Drinking-Water Quality, fourth ed. WHO Press, Geneva, Switzerland, p. 2011.

Wu, J., Wang, J., Li, H., Du, Y., Huang, K., Liu, B., 2013. Designed synthesis of hematite-based nanosorbents for dye removal. J. Mater. Chem. A 1, 9837–9847. https://doi.org/10.1039/c3ta11520h.

Zhou, H., Tan, Y., Gao, W., Zhang, Y., Yang, Y., 2020. Selective nitrate removal from aqueous solutions by a hydrotalcite-like absorbent FeMgMn-LDH. Sci. Rep. 10, 1–10. https://doi.org/10.1038/s41598-020-72845-3.